ResearchGate

See discussions, stats, and author profiles for this publication at: https://www.researchgate.net/publication/51908053

Preparation of Fe3O4@SiO2@Layered Double Hydroxide Core–Shell Microspheres for Magnetic Separation of Proteins

ARTICLE *in* JOURNAL OF THE AMERICAN CHEMICAL SOCIETY · DECEMBER 2011

Impact Factor: 12.11 · DOI: 10.1021/ja2086323 · Source: PubMed

CITATIONS
202

READS
150

6 AUTHORS, INCLUDING:

Mingfei Shao
Beijing University of Chemical Technology
25 PUBLICATIONS **727** CITATIONS
SEE PROFILE

Jingwen Zhao
Chinese Academy of Sciences, Qingdao, Qin…
20 PUBLICATIONS **630** CITATIONS
SEE PROFILE

Available from: Jingwen Zhao
Retrieved on: 24 January 2016

JACS
JOURNAL OF THE AMERICAN CHEMICAL SOCIETY

Article

pubs.acs.org/JACS

Preparation of Fe_3O_4@SiO_2@Layered Double Hydroxide Core–Shell Microspheres for Magnetic Separation of Proteins

Mingfei Shao, Fanyu Ning, Jingwen Zhao, Min Wei,* David G. Evans, and Xue Duan

State Key Laboratory of Chemical Resource Engineering, Beijing University of Chemical Technology, Beijing 100029, People's Republic of China

Supporting Information

ABSTRACT: Three-component microspheres containing an SiO_2-coated Fe_3O_4 magnetite core and a layered double hydroxide (LDH) nanoplatelet shell have been synthesized via an in situ growth method. The resulting Fe_3O_4@SiO_2@NiAl-LDH microspheres display three-dimensional core–shell architecture with flowerlike morphology, large surface area (83 m^2/g), and uniform mesochannels (4.3 nm). The Ni^{2+} cations in the NiAl-LDH shell provide docking sites for histidine and the materials exhibit excellent performance in the separation of a histidine (His)-tagged green fluorescent protein, with a binding capacity as high as 239 $\mu g/mg$. The microspheres show highly selective adsorption of the His-tagged protein from *Escherichia coli* lysate, demonstrating their practical applicability. Moreover, the microspheres possess superparamagnetism and high saturation magnetization (36.8 emu/g), which allows them to be easily separated from solution by means of an external magnetic field and subsequently reused. The high stability and selectivity of the Fe_3O_4@SiO_2@NiAl-LDH microspheres for the His-tagged protein were retained over several separation cycles. Therefore, this work provides a promising approach for the design and synthesis of multifunctional LDH microspheres, which can be used for the practical purification of recombinant proteins, as well as having other potential applications in a variety of biomedical fields including drug delivery and biosensors.

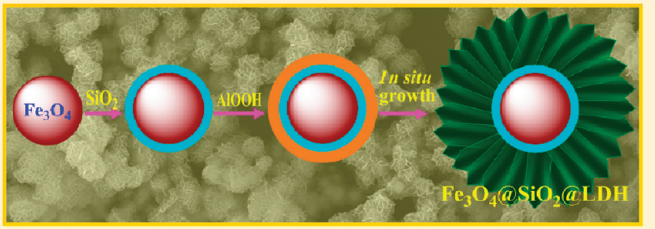

INTRODUCTION

With the ongoing need for purified proteins in applications ranging from diagnostics to therapeutics, the development of efficient methods for the separation and purification of recombinant proteins is increasingly essential in proteomics.[1] Traditionally, affinity chromatography with nickel(II) ions immobilized on a suitable column has been used to separate histidine (His)-tagged proteins from a matrix containing other undesirable biological elements. However, this technique generally suffers from high pressure drop, slow intrabead diffusion of solutes, and long separation time as well as difficult manipulations.[2] Several separation systems based on magnetic nanomaterials have been developed to avoid the disadvantages of such column-based systems, such as nitrilotriacetic acid (NTA)[3] or polymer brush-modified magnetic nanoparticles,[4] Au–Ni–Au triblock nanorods,[5] Ni/NiO core–shell nanoparticles,[6] and Fe_2O_3/SiO_2 core–shell microspheres decorated with NiO nanoparticles.[7] These approaches, however, still suffer from drawbacks such as low magnetic moments and leaching of NiO, as well as poor recyclability, which restrict their practical application in protein separation. Therefore, it is necessary to develop new approaches to fabricate magnetic separation systems for proteins, based on materials with appropriate magnetic properties, high capacity, and good recyclability.

Layered double hydroxides (LDHs) are a large class of inorganic layered materials that have been widely used in the fields of catalysis,[8] separation,[9] biology, and medicine.[10] However, conventional methods for LDH preparation give poor control over the morphology, particle size, and surface area and are unable to prevent aggregation of powder samples; this significantly limits the applications of the resulting materials as catalysts and adsorbents. From this view of point, hierarchical structures with controllable morphology, orientation, and dimensionality have evoked considerable interest owing to their superior properties. Recent attention has focused on the fabrication of LDHs with well-defined 2D or 3D nanostructures as a strategy to enhance their potential for practical applications. To date, although several types of ordered LDH structures have been developed (e.g., functional ultrathin films,[11] 3D macroporous LDHs,[12] and core–shell or hollow spheres[13]), many problems still remain unresolved. First, LDHs with a monodisperse, narrow particle size distribution as well as tunable topology and composition have not been successfully achieved. Second, to meet specific requirements for applications such as targeted drug delivery or efficient separation of biomaterials, the assembly of sophisticated LDH-containing architectures combined with other functional components is required, which is very demanding. Therefore, it is still a challenge to fabricate the type of multifunctional LDH materials with a hierarchical

Received: September 16, 2011

 © XXXX American Chemical Society dx.doi.org/10.1021/ja2086323 | J. Am. Chem.Soc. XXXX, XXX, XXX–XXX

structure which can be applied in adsorption as well as separation of biological molecules.

Herein, we report a facile and efficient synthesis of LDH microspheres (~600 nm in diameter) consisting of a silica-coated magnetite core (~300 nm in diameter) and an ordered shell of LDH nanoplatelets via a layer-by-layer (LBL) deposition process followed by an in situ growth technique, and demonstrate their application in the magnetic separation of a protein. The use of an in situ growth method allows the LDH nanoplatelets to become strongly and uniformly anchored onto the surface of the magnetic core. A series of core–shell Fe_3O_4@SiO_2@M(II)Al-LDH (M = Ni, Co, Zn, Mg) have been prepared with fine control over the shell thickness and composition. The efficiency of the Fe_3O_4@SiO_2@NiAl-LDH microspheres as affinity templates for the magnetic separation of proteins has been assessed by use of histidine (His)-tagged green fluorescent protein (GFP) as a probe. In addition, the stability, selectivity, and recyclability of the Fe_3O_4@SiO_2@NiAl-LDH microspheres were examined over several separation cycles, in order to investigate their potential as candidates for practical application in facile, efficient, and cost-effective bioseparation.

EXPERIMENTAL DETAILS

Synthesis of Fe_3O_4@SiO_2@LDH Microspheres. The synthesis procedure involves (1) preparation of uniform magnetite (Fe_3O_4) microspheres; (2) preparation of Fe_3O_4@SiO_2 structures via a sol–gel approach; (3) deposition of AlOOH on the surface of Fe_3O_4@SiO_2 spheres by the layer-by-layer (LBL) method (giving a material designated as Fe_3O_4@SiO_2@AlOOH); and (4) growth of LDH nanoplatelets on the surface of Fe_3O_4@SiO_2@AlOOH by an in situ growth technique through transformation of AlOOH into LDH (denoted as Fe_3O_4@SiO_2@LDH) by reaction with a solution containing the appropriate M^{2+} ions. The whole process is shown in Scheme 1. The synthesis details are as follows:

Scheme 1. Schematic Illustration of Fabrication of Fe_3O_4@SiO_2@LDH Microspheres

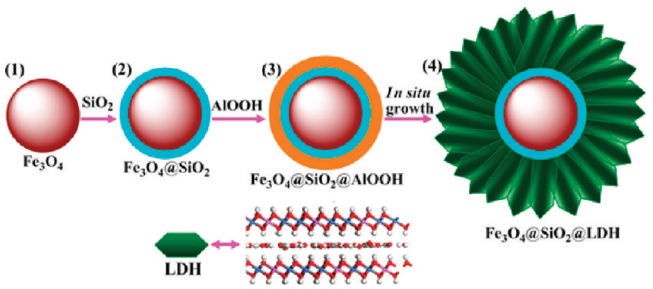

Synthesis of Fe_3O_4 Particles. The magnetic particles were prepared by means of a solvothermal reaction as reported previously.[14] Briefly, 2.70 g of $FeCl_3{\cdot}6H_2O$ and 7.20 g of sodium acetate were dissolved in 100 mL of ethylene glycol under vigorous stirring. The resulting homogeneous yellow solution was transferred to a Teflon-lined stainless-steel autoclave, sealed, and heated at 200 °C. After the reaction was allowed to proceed for 8 h, the autoclave was cooled to room temperature. The resulting black magnetite particles were washed several times with ethanol and dried in vacuum at 60 °C for 12 h. The magnetite particles were ~300 nm in diameter.

Synthesis of Fe_3O_4@SiO_2 Microspheres. The core–shell Fe_3O_4@SiO_2 microspheres were prepared according to a previously reported method.[15] Typically, 0.10 g of Fe_3O_4 particles was treated with 0.1 M HCl aqueous solution (50 mL) by ultrasonication for 10 min. The magnetite particles were separated, washed with deionized water, and homogeneously dispersed in a mixture of ethanol (80 mL), deionized water (20 mL), and concentrated ammonia aqueous solution (1.0 mL, 28 wt %), followed by the addition of tetraethyl orthosilicate (TEOS; 0.03 g, 0.144 mmol). After being stirred at room temperature for 6 h, the Fe_3O_4@SiO_2 microspheres were separated, washed with ethanol and water, and then dried in vacuum at 60 °C for 6 h.

Preparation of Fe_3O_4@SiO_2@AlOOH Microspheres. First, the AlOOH primer sol was prepared according to the method reported by our group.[16] Typically, aluminum isopropoxide ($Al(OPr)_3$) (11.3 g) was dissolved in 100 mL of deionized water by stirring at 85 °C for 20 min. HNO_3 (1.0 M) was then slowly added dropwise to the solution to initiate the hydrolysis of $Al(OPr)_3$, with the solution pH held in the range 3–4. The mixture was stirred at 85 °C for 2 h and then slowly cooled to room temperature, and solid boehmite (AlOOH) was obtained after evaporation of water. After milling, the boehmite (5.8 g) was added to 107 mL of deionized water with stirring at 85 °C for 1 h. Then HNO_3 (9.5 mL, 1.0 M) was slowly added dropwise to the solution, which was refluxed gently with stirring for 6 h. The AlOOH primer sol was obtained after slow cooling to room temperature. Subsequently, the Fe_3O_4@SiO_2 microspheres were dispersed in the AlOOH primer sol for 1 h with vigorous agitation, followed by withdrawing the microspheres with a magnet and then washing them thoroughly with ethanol. The resulting Fe_3O_4@SiO_2@AlOOH microspheres were dried in air for 30 min. The whole process (dispersion, withdrawing, drying) was repeated 10 times.

Preparation of Fe_3O_4@SiO_2@LDH Microspheres. An in situ crystallization of a NiAl-LDH nanoplatelet shell on the surface of Fe_3O_4@SiO_2@AlOOH microspheres was carried out. In a typical procedure, 0.01 mol of $Ni(NO_3)_2{\cdot}6H_2O$ and 0.015 mol of NH_4NO_3 were dissolved in deionized water to form a solution with a total volume of 70 mL. The Fe_3O_4@SiO_2@AlOOH microspheres (0.1 g) were placed in the above solution in an autoclave at 100 °C for 48 h. Finally, the resulting Fe_3O_4@SiO_2@LDH microspheres were separated by a magnet, rinsed with ethanol, and dried at room temperature. Synthesis details for other M(II)Al-LDH (M = Co, Zn, Mg) microspheres are described in the Supporting Information.

Protein Binding and Separation. *Reaction of Fe_3O_4@SiO_2@NiAl-LDH Microspheres with Proteins.* Fe_3O_4@SiO_2@NiAl-LDH microspheres (1 mg) were added into a phosphate-buffered saline (PBS) solution containing His-tagged GFP (His-tagged GFP, 300 μg/mL; PBS, 0.15 M; pH = 7.4; V = 0.8 mL) and incubated with shaking for different times. The microspheres were subsequently isolated from the supernatant by use of a magnet, added to an imidazole solution (0.1 g/mL, 0.8 mL), and incubated with shaking to release the protein captured by the microspheres.

Expression and Purification of His-Tagged Proteins from Cell Lysate. A 200 mL portion of BL21(DE3) cells expressing His-GFP was grown to OD_{600} (optical density of the sample measured at 600 nm) = 0.6–0.8, induced with 0.2 mM isopropyl β-D-1-thiogalactopyranoside (IPTG) at 37 °C for 3.5 h, pelleted by centrifugation, and finally redispersed in 20 mL of PBS (pH = 7.0). After disruption of the cells by sonication, soluble fractions were obtained by centrifugation (12 000 rpm) at 4 °C for 10 min. The resulting fractions were incubated with 3 mg of Fe_3O_4@SiO_2@NiAl-LDH microspheres at room temperature for 30 min with shaking. The microspheres were separated by a magnet and washed twice with PBS (0.15 M PBS, pH = 7.0) to remove nonspecifically adsorbed lysates. Subsequently, the sample was added to an imidazole solution (20 mL, 0.1 g/mL) and incubated for 30 min to release His-tagged GFP from the Fe_3O_4@SiO_2@NiAl-LDH microspheres. The recovered His-tagged GFP was resolved by 12% sodium dodecyl sulfate– polyacrylamide gel electrophoresis (SDS–PAGE), and the gel was stained with Coomassie blue.

Sample Characterization. Powder X-ray diffraction patterns of the core–shell microsphere samples were collected on a Shimadzu XRD-6000 diffractometer by use of a Cu Kα source, with a scan step of 0.02° and a scan range between 3° and 80°. X-ray photoelectron spectra (XPS) were recorded on a Thermo VG Escalab 250 X-ray photoelectron spectrometer at a pressure of about 2×10^{-9} Pa with Al Kα X-rays as the excitation source. The morphology of the microspheres was investigated by use of a scanning electron

dx.doi.org/10.1021/ja2086323 | J. Am. Chem.Soc. XXXX, XXX, XXX–XXX

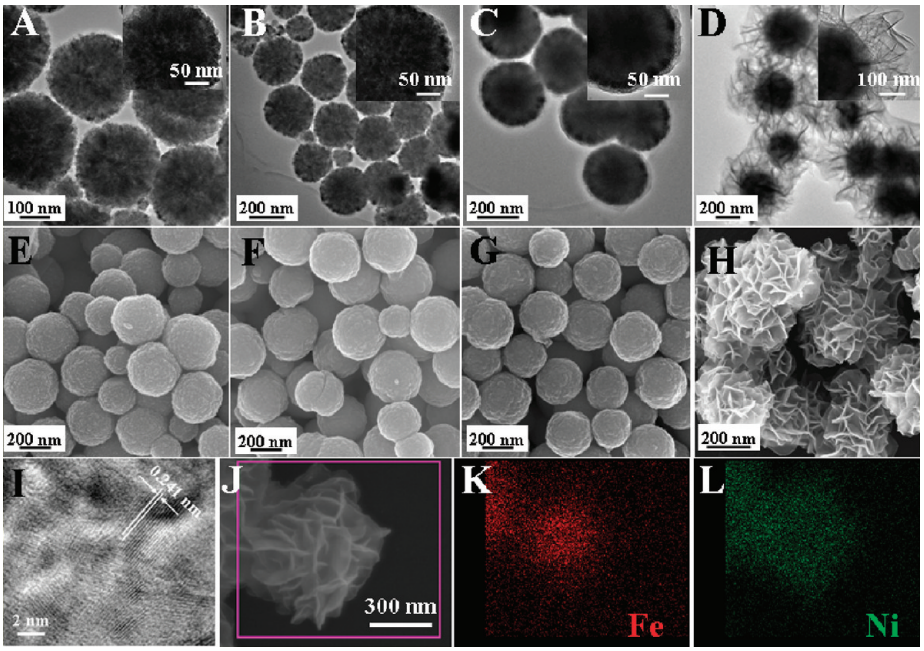

Figure 1. TEM and SEM images of (A, E) Fe_3O_4 particles, (B, F) Fe_3O_4@SiO_2, (C, G) Fe_3O_4@SiO_2@AlOOH, and (D, H) Fe_3O_4@SiO_2@NiAl-LDH microspheres. Also shown are (I) HR-TEM image of the NiAl-LDH shell and (J–L) EDX mapping results of a single Fe_3O_4@SiO_2@NiAl-LDH microsphere, demonstrating the Fe_3O_4 core/NiAl-LDH shell structure.

microscope (SEM; Zeiss SUPRA 55) with an accelerating voltage of 20 kV, combined with energy-dispersive X-ray spectroscopy (EDX) for determination of metal composition. Transmission electron microscopy (TEM) images were recorded with Philips Tecnai 20 and JEOL JEM-2010 high-resolution transmission electron microscopes. The accelerating voltage was 200 kV in each case. The specific surface area determination and pore volume and size analysis were performed by Brunauer–Emmett–Teller (BET) and Barrett–Joyner–Halenda (BJH) methods, respectively, by use of a Quantachrome Autosorb-1C-VP analyzer. Prior to the measurements, the samples were degassed at 100 °C for 6 h. The magnetic properties of the microspheres were measured on a LDJ 9600 vibrating sample magnetometer at room temperature. The fluorescence spectra were recorded on a Shimadzu RF-5301PC spectrofluorometer with an excitation wavelength of 400 nm; both the excitation and emission slits were 3.0 nm. Fluorescence of the samples was observed on an Olympus BX51 fluorescence microscope.

■ RESULTS AND DISCUSSION

Structural and Morphological Characterization. The Fe_3O_4 particles were prepared via a solvothermal method as described above. The TEM image shows that the Fe_3O_4 particles have a mean diameter of ~300 nm (Figure 1A). After being coated with a nonporous silica layer, core–shell Fe_3O_4@SiO_2 microspheres with a thin silica layer ~10 nm in thickness were obtained (Figure 1B, inset). The subsequent LBL deposition process resulted in a continuous and uniform AlOOH coating on the surface of Fe_3O_4@SiO_2 microspheres (~15 nm in thickness) (Figure 1C). Figure 1 panels E, F, and G display typical SEM images of Fe_3O_4, Fe_3O_4@SiO_2, and Fe_3O_4@SiO_2@AlOOH microspheres respectively, illustrating that the products are all well-dispersed with near-spherical morphology. By an in situ growth procedure, a shell of NiAl-LDH was formed by reaction of the AlOOH coating deposited on the surface of Fe_3O_4@SiO_2 with an aqueous solution of a Ni^{2+} salt. The TEM image of the resulting Fe_3O_4@SiO_2@NiAl-LDH microspheres (Figure 1D) shows that they are composed of a compact core (~300 nm in diameter) and a lower density shell (~150 nm in thickness). The SEM image also shows that the flowerlike microspheres are uniform in both size and shape, with each LDH nanoplatelet perpendicularly grafted to the solid core so that the external surface of the microspheres is composed of the edges of the platelets (Figure 1H, Figure S1 in Supporting Information). The high-resolution transmission electron microscopy (HR-TEM) image shows lattice fringes corresponding to an interplanar distance of ~0.24 nm that can be attributed to the (012) plane of a NiAl-LDH phase (Figure 1I). EDX mapping analysis is shown in Figure 1J–L, from which it can be observed that the iron is located in the central part of the particle while nickel is homogeneously distributed throughout the whole microsphere. The EDX spectrum of the microspheres (Figure S2, Supporting Information) also shows the presence of Ni, Al, and Fe (with a Ni/Al molar ratio of ~4.0), which is consistent with the mapping results. In addition, Fe_3O_4@SiO_2@M(II)Al-LDH (M = Co, Zn, Mg) microspheres were also synthesized via the in situ growth method by changing the divalent metal precursor, giving materials with a similar uniform flowerlike morphology and narrow particle size distribution (Co, ~600 nm; Zn, ~650 nm; Mg, ~500 nm) with LDH nanoplatelets perpendicular to the core (Figure S3, Supporting Information). In addition, the M(II)/Al ratios of the Fe_3O_4@SiO_2@M(II)Al-LDH (M = Ni, Co, Zn, Mg) materials were obtained by elemental analysis (inductively coupled plasma–atomic emission spectroscopy, ICP-AES), and the values are listed in Table S1 (Supporting Information).

It is worth mentioning that the Fe_3O_4@SiO_2@LDH core–shell microspheres cannot be obtained in the absence of the AlOOH layer on the surface of Fe_3O_4@SiO_2 (Figure S4A; see Supporting Information for detailed procedure). This confirms that the AlOOH coating plays a key role in providing the necessary aluminum source for the growth of ordered LDH nanocrystals. Moreover, it was found that without the SiO_2 layer between Fe_3O_4 and AlOOH the LDH nanoplatelets did

dx.doi.org/10.1021/ja2086323 | J. Am. Chem.Soc. XXXX, XXX, XXX–XXX

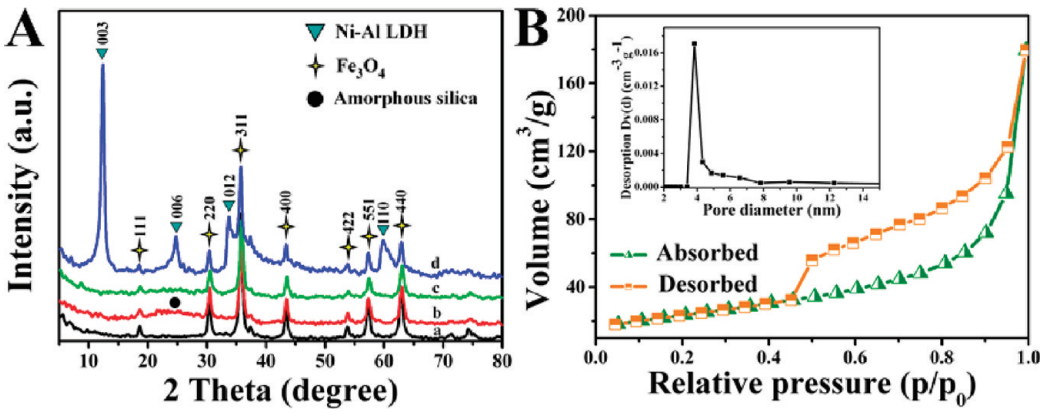

Figure 2. (A) XRD patterns of (a) Fe_3O_4, (b) Fe_3O_4@SiO_2, (c) Fe_3O_4@SiO_2@AlOOH, and (d) Fe_3O_4@SiO_2@NiAl-LDH microspheres. (B) N_2 sorption isotherms and pore size distribution (inset) of Fe_3O_4@SiO_2@NiAl-LDH microspheres.

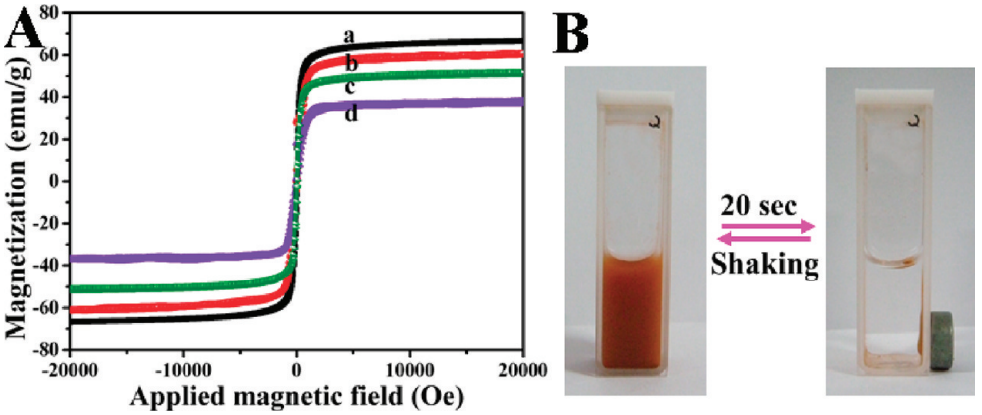

Figure 3. (A) Room-temperature (300 K) magnetic hysteresis loops of (a) Fe_3O_4, (b) Fe_3O_4@SiO_2, (c) Fe_3O_4@SiO_2@AlOOH, and (d) Fe_3O_4@SiO_2@NiAl-LDH microspheres. (B) Magnetic separation−redispersion process of Fe_3O_4@SiO_2@Ni−Al LDH microspheres.

not grow well (Figure S4B, Supporting Information), forming only a thin layer of LDH (~40 nm), which is likely to have poor adsorption and separation abilities. The introduction of the SiO_2 layer possibly facilitates the firm immobilization of the AlOOH coating owing to the hydrogen-bonding interactions between them.

Figure 2A shows the XRD patterns of Fe_3O_4, Fe_3O_4@SiO_2, Fe_3O_4@SiO_2@AlOOH, and Fe_3O_4@SiO_2@NiAl-LDH. The diffraction peaks in curve a can be indexed as a face-centered cubic (fcc) Fe_3O_4 phase (JCPDS card 19-629). After coating with the silica layer, the diffraction pattern of the resulting material (curve b) shows a reflection characteristic of amorphous SiO_2 in addition to the Fe_3O_4 reflections. The XRD pattern of the Fe_3O_4@SiO_2@AlOOH microspheres (curve c) is very similar to that of the Fe_3O_4@SiO_2, indicating the amorphous nature of the boehmite coating. The XRD pattern of the resulting Fe_3O_4@SiO_2@NiAl-LDH microspheres (curve d) after the in situ growth process exhibits the superimposition of reflections of a Fe_3O_4 phase and an LDH phase. The (003), (006), (012), and (110) reflections of a typical LDH material are clearly observed, indicating the high crystallinity of the product. The Fourier transform infrared (FT-IR) spectrum of Fe_3O_4@SiO_2@NiAl-LDH microspheres (Figure S5, Supporting Information) shows the presence of cyanate (CNO^-) anion in the interlayer region of NiAl-LDH, originating from the incomplete hydrolysis of urea in the in situ growth process of LDH shell.[17]

The specific surface area and porosity of the as-prepared M(II)Al-LDH (M = Ni, Co, Zn, Mg) microspheres were determined by nitrogen sorption measurements. Figure 2B displays the N_2 adsorption−desorption isotherms and the corresponding pore-size distribution curve for Fe_3O_4@SiO_2@NiAl-LDH microspheres. The core−shell microspheres exhibit a typical IV isotherm with a H3-type hysteresis loop (P/P_0 > 0.4), indicating the presence of mesopores. This result is further confirmed by the well-developed mesopores with a diameter of 4.2 nm in the pore size distribution plot, as shown in the inset of Figure 2B. The core−shell Fe_3O_4@SiO_2@NiAl-LDH microspheres have a specific surface area of 83.3 m^2/g, which is close to those of Fe_3O_4@SiO_2@CoAl-LDH (78.4 m^2/g), Fe_3O_4@SiO_2@ZnAl-LDH (75.3 m^2/g), and Fe_3O_4@SiO_2@MgAl-LDH (80.1 m^2/g) microspheres (shown in Figure S6 in Supporting Information).

Magnetic characterization at 300 K with a vibrating sample magnetometer showed that the saturation magnetization values of Fe_3O_4, Fe_3O_4@SiO_2, Fe_3O_4@SiO_2@AlOOH, and Fe_3O_4@SiO_2@NiAl-LDH microspheres were 80.7, 78.0, 53.3, and 36.8 emu/g (Figure 3A; see Figure S7 in Supporting Information for the expanded hysteresis loop), respectively. The magnified hysteresis loops further confirm the superparamagnetism of these particles. The Fe_3O_4@SiO_2@NiAl-LDH microspheres can be dispersed in water by vigorous shaking or sonication, resulting in a brown-colored suspension. Very fast aggregation of the microspheres from their homogeneous dispersion was observed in the presence of an external magnetic field, while

dx.doi.org/10.1021/ja2086323 | J. Am. Chem.Soc. XXXX, XXX, XXX−XXX

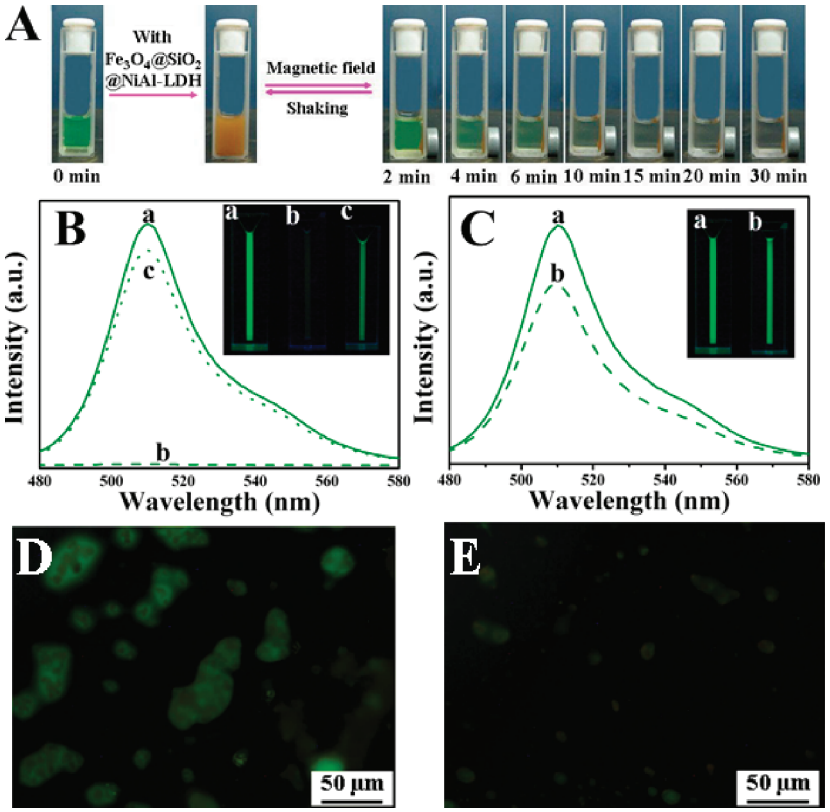

Figure 4. (A)Photographs of separation of His-tagged GFP by Fe_3O_4@SiO_2@NiAl-LDH microspheres after different times. (B) Fluorescence spectra of His-tagged GFP solution: (a) original solution, (b) after reaction with Fe_3O_4@SiO_2@NiAl-LDH microspheres for 20 min, (c) released His-tagged GFP solution. (C) Fluorescence spectra of GFP solution without a His tag: (a) original solution, (b) after reaction with Fe_3O_4@SiO_2@NiAl-LDH microspheres for 20 min.(D, E) Fluorescence microscopic images of (D) His-tagged GFP/microspheres and (E) GFP/microspheres.

redispersion occurred quickly with a slight shaking once the magnetic field was removed (Figure 3B). These results show that Fe_3O_4@SiO_2@NiAl-LDH microspheres possess excellent magnetic responsivity and redispersibility, which is important in terms of their practical manipulation.

Application in Protein Separation. The protein separation efficiency of Fe_3O_4@SiO_2@NiAl-LDH microspheres was investigated by following their reaction with His-tagged GFP. The magnetic Fe_3O_4@SiO_2@NiAl-LDH microspheres were incubated in a His-tagged GFP solution at room temperature for different times and then separated from the solution by applying a magnet. The release of the His-tagged GFP was carried out by incubating the microspheres in an imidazole solution, as shown in Scheme S1 (Supporting Information). Figure 4A shows photographs of the separation process after different reaction times. The solution color gradually fades from green to colorless after 20 min, indicating fast and almost complete adsorption of His-tagged GFP by the Fe_3O_4@SiO_2@NiAl-LDH microspheres. The fluorescence emission intensity of the supernatant solution (curve a, Figure 4B) decreases to essentially zero after 20 min (curve b, Figure 4B), confirming that the microspheres efficiently bind His-tagged GFP. Incubation of His-tagged GFP/microspheres in a concentrated imidazole solution induces dissociation of the protein from the microspheres, resulting in recovery of 90% of the initial fluorescence emission intensity (curve c, Figure 4B). As a control experiment, when GFP without a His tag was reacted with Fe_3O_4@SiO_2@NiAl-LDH microspheres under identical conditions, a decrease in the fluorescence emission intensity of only 24% was observed for the supernatant (from curve a to curve b, Figure 4C), indicating a weak interaction between GFP and microspheres. The fluorescence microscopic image of His-tagged GFP/microspheres after magnetic separation shows strong green fluorescence (Figure 4D), whereas extremely weak green emission was observed for GFP/microspheres (Figure 4E), confirming the selective attachment of His-tagged protein to the surface of Fe_3O_4@SiO_2@NiAl-LDH microspheres.

To better understand the interaction between NiAl-LDH microspheres and His-tagged protein, a fine-scan XPS of the Ni region was performed for Fe_3O_4@SiO_2@NiAl-LDH microspheres before and after reaction with His-tagged GFP, as shown in Figure 5. For as-prepared Fe_3O_4@SiO_2@NiAl-LDH microspheres, the measured binding energies of Ni $2p_{3/2}$ and Ni $2p_{1/2}$ are 855.6 and 873.1 eV, respectively (Figure 5, curve a). The energy difference between them is ~17.5 eV, which is close to that of NiAl-LDH.[18] Moreover, the appearance of satellite peaks (labeled "sat") implies the presence of a high-spin divalent state of Ni^{2+} in the sample.[19] However, the XPS spectrum exhibits a significant change after reaction with His-tagged GFP for 20 min (Figure 5, curve b). The binding energies of Ni $2p_{3/2}$ and Ni $2p_{1/2}$ shift to 855.1 and 872.7 eV, respectively, suggesting there is an interaction between Ni^{2+} in the LDH platelets and His tag. In addition, the XPS spectra of Al and Fe do not show any significant changes (Figure S8, Supporting Information), which indicates that only Ni^{2+} has a specific interaction with the His tag in the Fe_3O_4@SiO_2@NiAl-LDH system.

The performance of Fe_3O_4@SiO_2@NiAl-LDH microspheres in the separation of His-tagged proteins was compared with those of MgAl-, ZnAl-, and CoAl-LDH microspheres. As shown

dx.doi.org/10.1021/ja2086323 | J. Am. Chem.Soc. XXXX, XXX, XXX–XXX

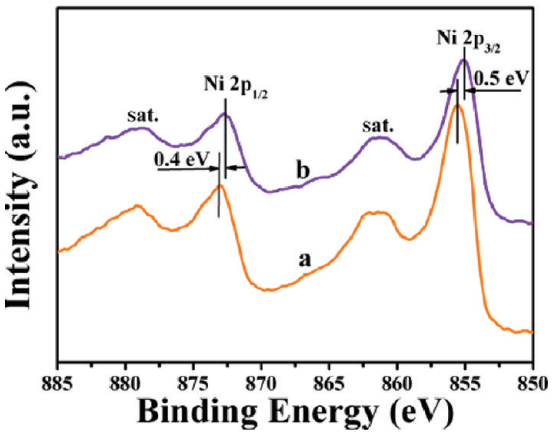

Figure 5. Typical Ni 2p XPS spectra for Fe_3O_4@SiO_2@NiAl-LDH microspheres (a) before and (b) after reaction with His-tagged GFP.

in Figure S9 in Supporting Information, in each case the fluorescence emission intensity of the His-tagged GFP solution decreased after reaction with the LDH microspheres for 30 min, with the magnitude of the change in emission intensity decreasing in the order NiAl > CoAl > ZnAl > MgAl. This was further confirmed by photographs of the corresponding His-tagged GFP solution after reaction with different LDH microspheres (Figure S10, Supporting Information) and plots of the binding capacity versus reaction time (Figure S11, Supporting Information). After 30 min, the NiAl-LDH microspheres exhibited a binding capacity for His-tagged GFP of 239 μg/mg, much larger than that of CoAl-LDH, ZnAl-LDH, and MgAl-LDH. No correlation between adsorption capacity and surface charge density can be found on the basis of M(II)/Al ratio (Table S1, Supporting Information) and ζ potential analysis (Figure S12, Supporting Information), indicating that electrostatic interaction is not the key factor in determining the adsorption behavior of these LDH microspheres. In addition, the specific surface areas of the four samples are rather close (Figure 2B and Figure S6 in Supporting Information), which excludes the influence of nonspecific interactions. Since the formation constants for complexation with histidine also decrease[20] in the order Ni^{2+} > Co^{2+} > Zn^{2+} > Mg^{2+}, the data suggest that the His tag becomes coordinated by exposed M^{2+} ions at the edges of the LDH platelets rather than simply being nonspecifically adsorbed on the surface, consistent with the XPS data showing that there is an interaction between Ni^{2+} and histidine.

The recyclability of the Fe_3O_4@SiO_2@NiAl-LDH microspheres was also tested. As shown in Figure 6A, the binding capacity of the microspheres to His-tagged GFP was almost unchanged (~232 μg/mg) after five cycles of reuse, and the release percentage also remained essentially unchanged. This can be attributed to the core−shell hierarchical structure of Fe_3O_4@SiO_2@NiAl-LDH microspheres, which provides both docking sites for His-tagged protein (the NiAl-LDH shell) and a superparamagnetic core allowing easy manipulation by a magnetic field. In addition, the morphology of the Fe_3O_4@SiO_2@NiAl-LDH microspheres remains unchanged after five cycles (Figure S13, Supporting Information), indicating that the material is robust.

To demonstrate an actual practical application of Fe_3O_4@SiO_2@NiAl-LDH microspheres, they were incubated in an *E. coli* cell lysate containing His-GFP proteins and then separated by use of a magnetic field. SDS−PAGE analysis showed that

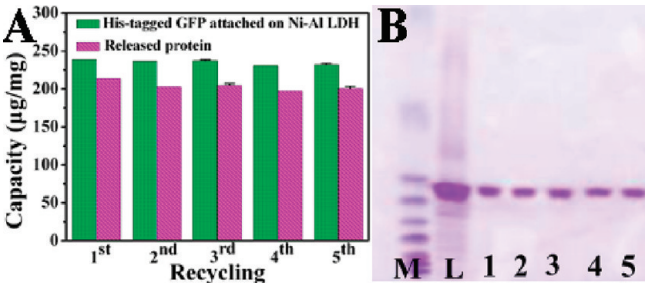

Figure 6. (A) Magnetic separation and recycling of Fe_3O_4@SiO_2@NiAl-LDH microspheres in the separation of His-tagged GFP. (B) SDS−PAGE analyses of cell lysate containing His-GFP (lane L) and proteins released from the Fe_3O_4@SiO_2@NiAl-LDH microspheres reused up to five times (lanes 1−5). Lane M is a molecular weight marker.

the His-tagged GFP was efficiently separated by the microspheres (lane 1, Figure 6B). In addition, the affinity and specificity of Fe_3O_4@SiO_2@NiAl-LDH microspheres remained unaffected after being recovered and reused up to five times, as shown in Figure 6B (lanes 2−5). Therefore, the Fe_3O_4@SiO_2@NiAl-LDH microspheres show good selectivity and recyclability for the separation of His-tagged proteins in the *E. coli* lysate.

CONCLUSIONS

Fe_3O_4@SiO_2@LDH microspheres can be synthesized by in situ growth of LDH nanoplatelets on the surface of magnetic nanospheres. The microspheres exhibit a three-dimensional core−shell architecture and large surface area and can be used for the efficient magnetic separation of His-tagged proteins since the NiAl-LDH shell provides abundant docking sites for the His-tagged protein via the binding between Ni^{2+} and the His tag. Furthermore, the presence of the superparamagnetic core in the microspheres allows them to be isolated by means of an external magnetic field, facilitating their recycling and reuse. Fe_3O_4@SiO_2@NiAl-LDH microspheres display high selectivity and stability for His-tagged GFP over several separation cycles. A practical application of the microspheres was successfully demonstrated in *E. coli* cell lysate containing His-GFP protein. Therefore, this work provides a facile and efficient approach for the fabrication of magnetic core/functionalized LDH shell hierarchical structures, which have potential applications in a variety of biomedical fields including protein separation and purification, drug delivery, and biosensors.

ASSOCIATED CONTENT

Supporting Information

Additional text, 13 figures, one table, and one scheme showing experimental details of preparation of Fe_3O_4@SiO_2@M(II)Al-LDH (M = Co, Zn, and Mg) microspheres; FT-IR spectra, EDS spectrum, low-resolution SEM images, and XPS spectra of Fe_3O_4@SiO_2@NiAl-LDH microspheres; N_2 sorption isotherms and pore size distribution of Fe_3O_4@SiO_2@M(II)Al-LDH (M = Co, Zn, and Mg) microspheres; ζ potential distribution spectra and composition of Fe_3O_4@SiO_2@M(II)Al-LDH (M = Ni, Co, Zn, and Mg) microspheres; and performance of Fe_3O_4@SiO_2@M(II)Al-LDH (M = Co, Zn, and Mg) microspheres in separation of His-tagged proteins. This material is available free of charge via the Internet at http://pubs.acs.org.

dx.doi.org/10.1021/ja2086323 | J. Am. Chem.Soc. XXXX, XXX, XXX−XXX

AUTHOR INFORMATION

Corresponding Author

weimin@mail.buct.edu.cn

ACKNOWLEDGMENTS

This project was supported by the National Natural Science Foundation of China, the 973 Program (Grant 2011CBA00504), and the Collaboration Project from the Beijing Education Committee.

REFERENCES

(1) (a) Arnau, J.; Lauritzen, C.; Peterson, G. E.; Pedersen. *J. Protein Expression Purif.* **2006**, *48*, 1−13. (b) Zhen, G.; Falconnet, D.; Kuennemann, E.; Voros, J.; Spencer, N. D.; Textor, M.; Zurcher, S. *Adv. Funct. Mater.* **2006**, *16*, 243−251. (c) Dyr, J. E.; Suttnar, J. *J. Chromatogr. B* **1997**, *699*, 383−401. (d) Mascagni, P.; Ball, H. L.; Bertolini, G. *Anal. Chim. Acta* **1997**, *352*, 375−385.

(2) (a) Jain, P.; Sun, L.; Dai, J. H.; Baker, G. L.; Bruening, M. L. *Biomacromolecules* **2007**, *8*, 3102−3107. (b) Zou, H.; Luo, Q.; Zhou, D. J. *Biochem. Biophys. Methods.* **2001**, *49*, 199−240. (c) Clairbois, A.-S.; Letourneur, D.; Muller, D.; Jozefonvicz, J. *J. Chromatogr. B* **1998**, *706*, 55−62.

(3) (a) Xu, C.; Xu, K.; Gu, H.; Zhong, X.; Guo, Z.; Zheng, R.; Zhang, X.; Xu, B. *J. Am. Chem. Soc.* **2004**, *126*, 3392−3393. (b) Xu, C.; Xu, K.; Gu, H.; Zheng, R.; Liu, H.; Zhang, X.; Guo, Z.; Xu, B. *J. Am. Chem. Soc.* **2004**, *126*, 9938−9939.

(4) Geiger, J. H.; Baker, G. L.; Bruening, M. L. *Langmuir* **2011**, *27*, 3106−3112.

(5) (a) Lee, K.-B.; Park, S.; Mirkin, C. A. *Angew. Chem., Int. Ed.* **2004**, *43*, 3048−3050. (b) Oh, B.-K.; Park, S.; Millstone, J. E.; Lee, S. W.; Lee, K.-B.; Mirkin, C. A. *J. Am. Chem. Soc.* **2006**, *128*, 11825−11829.

(6) Lee, I. S.; Lee, N.; Park, J.; Kim, B. H.; Yi, Y.-W.; Kim, T.; Kim, T. K.; Lee, I. H.; Paik, S. R.; Hyeon, T. *J. Am. Chem. Soc.* **2006**, *128*, 10658−10659.

(7) Kim, J.; Piao, Y.; Lee, N.; Park, Y.; Il; Lee, I.-H.; Lee, J.-H.; Paik, S. R.; Hyeon, T. *Adv. Mater.* **2010**, *22*, 57−60.

(8) (a) Sels, B.; Vos, D. D.; Buntinx, M.; Pierard, F.; Mesmaeker, K. D.; Jacobs, P. *Nature* **1999**, *400*, 855−857. (b) Choudary, B. M.; Kantam, M. L.; Rahman, A.; Reddy, C. V.; Rao, K. K. *Angew. Chem., Int. Ed.* **2001**, *40*, 763−766.

(9) (a) Fogg, A. M.; Green, V. M.; Harvey, H. G.; O'Hare, D. *Adv. Mater.* **1999**, *11*, 1466−1469. (b) Khan, A. I.; O'Hare, D. *J. Mater. Chem.* **2002**, *12*, 3191−3198.

(10) (a) Choy, J.-H.; Kwak, S.-Y.; Park, J.-S.; Jeong, Y.-J.; Portier, J. *J. Am. Chem. Soc.* **1999**, *121*, 1399−1400. (b) Gu, Z.; Thomas, A. C.; Xu, Z. P.; Campbell, J. H.; Lu, G. Q. *Chem. Mater.* **2008**, *20*, 3715−3722.

(11) (a) Han, J. B.; Dou, Y. B.; Wei, M.; Evans, D. G.; Duan, X. *Angew. Chem., Int. Ed.* **2010**, *49*, 2171. (b) Liu, Z. P.; Ma, R. Z.; Osada, M.; Iyi, N.; Ebina, Y.; Takada, K.; Sasaki, T. *J. Am. Chem. Soc.* **2006**, *128*, 4872−4880. (c) Shao, M. F.; Wei, M.; Evans, D. G.; Duan, X. *Chem. Commun.* **2011**, *47*, 3171−3173.

(12) (a) Géraud, E.; Prévot, V.; Ghanbaja, J.; Leroux, F. *Chem. Mater.* **2006**, *18*, 238−240. (b) Géraud, E.; Rafqah, S.; Sarakha, M.; Forano, C.; Prévot, V.; Leroux, F. *Chem. Mater.* **2008**, *20*, 1116−1125.

(13) (a) Gunawan, P.; Xu, R. *Chem. Mater.* **2009**, *21*, 781−783. (b) Pan, D.; Zhang, H.; Fan, T.; Chen, J.; Duan, X. *Chem. Commun.* **2011**, *47*, 908−910. (c) Li, L.; Feng, Y. J.; Li, Y. S.; Zhao, W. R.; Shi, J. L. *Angew. Chem., Int. Ed.* **2009**, *48*, 5888−5892.

(14) Xuan, S. H.; Wang, Y.-X. J.; Yu, J. C.; Leung, K. C.-F. *Langmuir* **2009**, *25*, 11835−11843.

(15) Deng, Y.; Qi, D.; Deng, C.; Zhang, X.; Zhao, D. *J. Am. Chem. Soc.* **2008**, *130*, 28−29.

(16) Zhao, Y.; He, S.; Wei, M.; Evans, D. G.; Duan, X. *Chem. Commun.* **2010**, *46*, 3031−3033.

(17) Shu, X.; Zhang, W. H.; He, J.; Gao, F. X.; Zhu, Y. X. *Solid State Sci.* **2006**, *8*, 634−639.

(18) Wei, M.; Xu, X. Y.; Wang, X. R.; Li, F.; Zhang, H.; Lu, Y. L.; Pu, M.; Evans, D. G.; Duan, X. *Eur. J. Inorg. Chem.* **2006**, 2831−2838.

(19) Huang, X. H.; Li, G. H.; Cao, B. Q.; Wang, M.; Hao, C. Y. *J. Phys. Chem. C* **2009**, *113*, 4381−4385.

(20) Pettit, L. D. *Pure Appl. Chem.* **1984**, *56*, 247−292.